Kinetic Calculations of the NTM Polarisation Current: Reduction for Small Island Widths and Sign Reversal Near the Diamagnetic Frequency

E. Poli[1], A. Bergmann[1], A. G. Peeters[1], L. Appel[2], S. D. Pinches[1]

[1]Max-Planck-Institut für Plasmaphysik, EURATOM Association, D-85748 Garching
[2]EURATOM/UKAEA Fusion Association, Culham Science Centre, Abingdon, Oxon, OX14 3DB, United Kingdom
e-mail: Emanuele.Poli@ipp.mpg.de

Abstract The polarisation current associated with a Neoclassical Tearing Mode is studied by means of drift kinetic δf simulations. This current has been invoked as a possible explanation for both the observed threshold for the minimum island size that can grow unstable and the scaling of the plasma pressure at the mode onset with the normalised gyroradius. The numerical approach presented in this paper does not require assumptions on the island size or the island rotation frequency, which are in contrast necessary in the analytic theory. The calculations are performed in toroidal geometry in the presence of a helical perturbation. In the case of an island width comparable to the ion banana width (typical for the early phase of a NTM) it turns out that the polarisation current decays linearly with decreasing island width. Moreover it is found that the sign of the polarisation current can flip for rotation frequencies close to the diamagnetic frequency. The kinetic effects mentioned above are not included in the present theory and must be considered in order to determine both sign and size of the polarisation-current contribution to the NTM evolution.

1. Introduction

The tearing mode [1,2] can be neoclassically destabilised in an otherwise tearing-stable plasma, as it has long been shown both theoretically [3,4] and experimentally [5,6]. In this case, the mode is driven unstable by the loss of bootstrap current inside an initial ("seed") magnetic island. The magnetic perturbation associated with this drop in the bootstrap current leads to a further growth of the island. The mode usually saturates when an equilibrium between the neoclassical driving mechanism and the stabilising influence of the current profile (expressed by a negative stability parameter Δ') is reached. A saturated Neoclassical Tearing Mode (NTM) causes a confinement degradation in today's fusion devices, and would reduce significantly the performance of ITER. At present, we can say that both the neoclassical growth and saturation of the NTM are well understood. However, predictions on the conditions under which the NTM will appear in ITER, and calculations about its possible stabilisation, are made difficult by the uncertanties about the physics determining the stability of "small" islands, i. e. islands with a size comparable to the seed-island size, as is the case in the early phase of the mode, or when the island width is reduced e.g. through localised curren drive [7]. In particular, it is often seen experimentally that the seed island must exceed a given threshold in order for the mode to become unstable. This is an indication that there must be some stabilising mechanism, acting at small island widths, that balances the neoclassical drive. Among the possible candidates discussed in the literature, the one which has probably received the most attention is the polarisation current connected with the time-dependent electric field associated with the rotation of the island with respect to the plasma [8,9]. Actually, whether this contribution to the evolution of the NTM is stabilising or destabilising is far from being clear (see Ref. [10] for a comprehensive summary). This is basically due to the fact that an accurate description of the physics determining the island rotation frequency is missing, so that the magnitude and even the sign of this frequency are still under debate. An interesting issue related to the polarisation current is the range of applicability of the existing theory in terms of allowed island (half-)width W. The drift kinetic theory of the island polarisation current in a toroidal geometry has been developed by Wilson et al. [9]. In this approach, the ion distribution function is expanded assuming

$$w_b/W \ll 1, \tag{1}$$

where $w_b = \sqrt{\varepsilon}\rho_p$ is the thermal ion banana width (ρ_p is the ion gyroradius calculated with the poloidal magnetic field). Moreover, in order to isolate the polarisation current from the contribution of the parallel ion streaming, it is assumed that

$$\omega \gg k_{\|} v_{\|}, \tag{2}$$

where ω is the island rotation frequency in the plasma rest frame, $v_{\|}$ is the particle velocity parallel to the magnetic field and $k_{\|} \sim (m/Rq)W/L_q$ is the parallel wave vector (m is the poloidal mode number of the resonant surface, R is the major radius and $L_q = (1/q)(\mathrm{d}q/\mathrm{d}r)$ is the scale length of the safety-factor profile q). Assuming $\omega \sim \omega_*$ and $L_n \approx L_q$, where ω_* is the diamagnetic frequency and L_n the scale length of the density profile, it is $\omega_*/k_{\|}v_{\|} = \rho_p/W$, so that the condition expressed by Eq.(2) is equivalent to $\rho_p \gg W$, consistently with the assumption that the polarisation current is important only for small islands. Summarising, the applicability of the existing kinetic theory is limited to the range $\sqrt{\varepsilon}\rho_p < W < \rho_p$.

It turns out, however, that under experimental conditions the assumption of Eq.(1) is violated. At the ASDEX Upgrade tokamak, for instance, typical values [11] for the thermal ion banana width range between about 0.7–3 cm, while the seed island that triggers the mode is in the range 1–5 cm. Hence, if the polarisation current plays a role in determining the size of the minimum seed island that can destibilise the NTM, the theoretical investigation has to be extended also below the range of Eq.(1). Indeed, if a trapped particle has an orbit whose size is comparable with the island size (which is also the typical scale associated with the island potential), one can expect that its behaviour will be different from that predicted on the basis of the above "local" assumption (1), according to which this particle does not see any variation of the potential during its bounce motion. This effect is supposed to be significant especially in the region around the island separatrix, where the potential changes rapidly.

Also an investigation of the polarisation current for frequencies which do not satisfy the condition expressed by Eq.(2) is necessary, since the actual value of ω is unknown, and the relevant physics in a full 3D geometry has not been considered so far.

To treat these phenomena in a realistic geometry, a numerical approach becomes necessary. Drift kinetic δf simulations of the polarisation current for a broad range of island rotation frequencies and in the "small-island" limit are the subject of this paper. It is shown that the relaxation of the assumptions (1,2) mentioned above leads to significant changes of the usual picture of the polarisation current.

2. Physical picture of the polarisation current in the presence of a rotaning island

Under experimental conditions, a magnetic island is in general rotating with respect to the surrounding plasma. As mentioned above, there exists still no reliable prediction of the island rotation frequency ω. This issue will not be addressed in this paper. The rotation frequency will be taken as a free parameter in the numerical simulations. The electrostatic potential associated with the island rotation, which determines the island polarisation current, is proportional to ω, cf. Eq.(3) below. In this Section, the potential which is used in the simulations is briefly derived and the resulting polarisation current is discussed.

In the presence of an island, the magnetic field $\mathbf{B}$ will be written as $\mathbf{B} = RB_t\nabla\varphi + \nabla\varphi \times \nabla(\psi + \tilde{\psi})$, where B_t is the equilibrium toroidal magnetic field, φ is the toroidal angle, ψ is the unperturbed poloidal flux and $\tilde{\psi} = \alpha\cos\xi = -RA_{\|}$ is the helical flux perturbation which describes the island. The helical angle $\xi \equiv m\theta - n\varphi - \omega t$ has been introduced, where m and n are the poloidal and toroidal numbers of the mode and θ is the poloidal angle. The quantity Ω defined as $\Omega \equiv 2(\psi-\psi_s)^2/W_\psi^2 - \cos\xi$ (the subscript s denotes evaluation at the resonant surface and $W_\psi^2 = 4\alpha q_s/q_s'$, where the prime indicates differentiation with respect to ψ) can then be used as a flux-surface label, since $\mathbf{B}\cdot\nabla\Omega = 0$. With this definition, $\Omega = -1$ corresponds to the O-point of the island, $\Omega = 1$ to the separatrix. It can be shown that the (poloidally averaged) gradient operator along $\mathbf{B}$ can be introduced as $\nabla_\| = k_\|\, \partial/\partial\xi|_\Omega$. The electrostatic potential can be obtained by supposing that the mobile electrons short-circuit the parallel electric field $E_\| = -\nabla_\|\Phi - (1/c)\partial A_\|/\partial t$. Using the identity $\partial A_\|/\partial\xi = (qk_\|/m)\partial\psi/\partial\xi|_\Omega$, the condition $E_\| = 0$ yields

$$\Phi = \frac{\omega q}{mc}\left[(\psi-\psi_s) - h(\Omega)\right], \tag{3}$$

where $h(\Omega)$ is a flux-surface function do be determined from the boundary conditions. It can be assumed that the electric field vanishes far away from the island, $h(\Omega) \to (\psi-\psi_s)$ if $|\psi-\psi_s| \gg W_\psi$. The simplest choice is then

$$h(\Omega) = \frac{W_\psi}{\sqrt{2}}\left(\sqrt{\Omega}-1\right)\Theta(\Omega-1). \tag{4}$$

Here W_ψ is defined to have the same sign as $\psi-\psi_s$, $\Omega = 1$ corresponds to the island separatrix and $\Theta(x)$ is the Heaviside function, which is introduced to be consistent with the quasi-neutrality condition and to ensure the flattening of the density profile inside the island, since it turns out that $n = n_s + n_s' h(\Omega)$.

The electric field $\mathbf{E} = -\nabla\Phi$ can be regarded as composed of two terms, cf. Eq.(3). The first one is proportional to the unperturbed flux ψ and leads to an $E\times B$ rotation of the whole plasma, mainly in the poloidal direction. The term proportional to $h(\Omega)$ vanishes inside the island and damps the electric field far away from it. In other words, the second term in Eq.(3) represents the potential in the island's rest frame, where the field has no explicit time dependence. In this reference system, the polarisation current can be understood more easily. The $E\times B$ flow is faster around the island O-point than around the X-point, cf. Fig. 1. The corresponding ac-

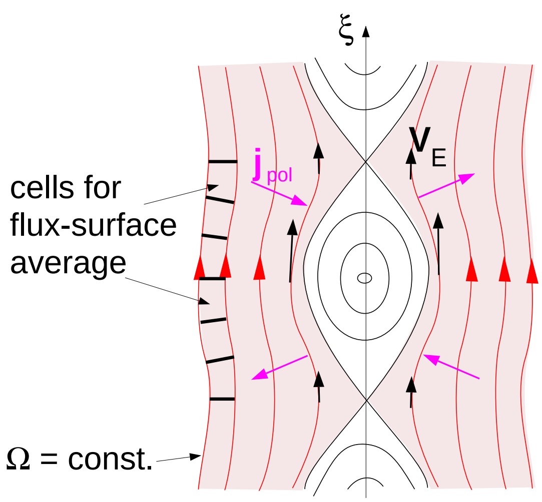

Figure 1: Polarisation current $j_{\rm pol}$ in the presence of a magnetic island.

celeration and deceleration of the plasma along the flux surfaces, $\rho\mathrm{d}\mathbf{v}/\mathrm{d}t$ (ρ is the mass density here) must be balanced by a Lorentz force $\mathbf{j}\times\mathbf{B}$, where the current is flowing perpendicular to the flux surfaces. This current is the classical polarisation current,

$$j_{\rm pol}^{\rm class} = \frac{en}{\omega_c}\frac{\mathrm{d}v_E}{\mathrm{d}t} = \frac{en}{\omega_c}\left(\mathbf{v}_E\cdot\nabla\right)v_E. \tag{5}$$

The picture is slightly more complicated in a toroidal device, where the poloidal rotation is neoclassically damped and a parallel flux $u_{\|} = cE/B_p$ develops in such a way that its poloidal component compensates the poloidal component of the $E \times B$ flow. The neoclassical polarisation current is then

$$j_{\rm pol}^{\rm nc} = \frac{en}{\omega_{cp}} (\mathbf{v}_E \cdot \nabla)\, u_{\|}, \tag{6}$$

which is a factor $B^2/B_p^2 = q^2/\varepsilon^2$ higher than the classical one, because in the latter case the flow that varies along the flux surface is a factor B/B_p larger than in the former case, and the corresponding acceleration in the Lorentz force must be provided by the poloidal component of the magnetic field. As is apparent from Eq.(6), the polarisation current is mainly carried by the ions, which have a larger inertia.

The motion of the particles carrying the neoclassical polarisation current has been investigated by Hinton and Robertson [12]. They have shown that a time-varying electric field modifies the orbits of the trapped particles in such a way that a net radial drift (much larger for the ions) is obtained. This drift is transferred collisionally to the untrapped particles, giving the neoclassical polarisation current as discussed above. In the case of a rotating island, however, if the collision frequency is smaller than the island rotation frequency, a trapped particle can drift radially back and forth several times before experiencing a collision, so that the collisional momentum transfer to the passing particles flux-averages to zero and the polarisation current is carried by the trapped ions alone. In this case the neoclassical enhancement factor is $q^2/\sqrt{\varepsilon}$, i.e. a factor $\varepsilon^{3/2}$ smaller than above. This will be the situation considered in the simulations presented in Sec. 4.

The polarisation current (perpendicular to $\mathbf{B}$) is closed by a parallel electron current to ensure charge neutrality. This parallel current contributes to the NTM evolution as described by the Rutherford equation, which is obtained by substituting $j_{\|}^{n.i.}$ into:

$$\frac{4\pi}{1.22\eta c^2}\frac{\mathrm{d}W}{\mathrm{d}t} = \frac{\Delta'}{2} + \frac{4\sqrt{2}}{c}\frac{qR}{sBW}\int_{-1}^{\infty}\mathrm{d}\Omega \oint \frac{\mathrm{d}\xi \cos\xi}{\sqrt{\cos\xi + \Omega}}\, j_{\|}^{n.i.}. \tag{7}$$

In Eq.(7), η is the neoclassical resistivity, Δ' is the usual stability parameter of the current profile [2], $s = (r/q)dq/dr$ is the magnetic shear (r being the minor radius). The contribution to $j_{\|}^{n.i.}$ due to the polarisation current is found to scale proportional to $1/W^2$, yielding a term proportional to $1/W^3$ in Eq.(7). This explains why the polarisation current is particularly important in the initial phase of the NTM, when the island width is small. The scaling $j_{\|}^{\rm pol} \propto 1/W^2$ is due to the fact that in $\nabla_{\|} j_{\|} = -\nabla_{\perp} \cdot \mathbf{j}_{\perp}$ one has $\nabla_{\|} \propto k_{\|} \propto W$ and $\nabla_{\perp} \propto 1/W$. The (perpendicular) polarisation current itself is independent of the island size because $\mathbf{v}_E$ and its derivative along the $\mathbf{v}_E$-direction do not depend on W, cf. Eq.(5) or Eq.(6). The limits of validity of the picture outlined in this section are discussed below on the basis of Monte Carlo δf solutions of the ion drift-kinetic equation.

3. The Monte Carlo δf approach

The calculation of the polarisation current for an arbitrary island width relies on the solution of the drift kinetic equation

$$\frac{\mathrm{d}f}{\mathrm{d}t} = \frac{\partial f}{\partial t} + \left(v_{\|}\hat{\mathbf{b}} + \mathbf{v}_d + \mathbf{v}_E\right)\cdot\frac{\partial f}{\partial \mathbf{r}} - \frac{e}{m_i}\frac{\mathbf{v}\cdot\nabla\Phi}{v}\frac{\partial f}{\partial v} = C(f) \tag{8}$$

in a toroidal geometry, including the presence of the island in the magnetic configuration. In Eq.(8), f is the ion distribution function, $\mathbf{v}_d$ and $\mathbf{v}_E$ are the magnetic and electric drift velocities,

e and m_i are the charge and the mass of the ions and C is the pitch-angle scattering operator. In this paper, the δf method is employed. The distribution function is written as the sum of a time-independent analytically-known bulk term f_0 and a deviation δf to be evaluated numerically. The equation for δf is then

$$\frac{\mathrm{d}(\delta f)}{\mathrm{d}t} = C(\delta f) - \mathbf{v}_d \cdot \nabla f_M - \frac{e f_M}{T}\mathbf{v}_d \cdot \nabla\Phi, \tag{9}$$

where the right-hand side of Eq. (9) represent the "source" which leads to a deviation from f_0, supposed here to be a Maxwellian f_M. The numerical scheme employed here is very close to that already used to study near-axis neoclassical transport [13] and bootstrap current in the presence of an island [11] and already described in detail. The evolution of the system is represented by means of "markers", which span the whole phase space. They evolve according to the equations of motion, which are integrated by means of the code HAGIS [14]. Collisions are implemented by means of a momentum-conserving Monte Carlo procedure [13].

The magnetic equilibrium is specified analytically to save computational time. The unperturbed magnetic surfaces are circular and concentric. A magnetic perturbation of given helicity can be superimposed as $\tilde{\psi} = \alpha \cos\xi$, where both the mode amplitude $\alpha \propto W^2$ and the mode rotation frequency ω (contained in ξ) are input parameters in the simulations. No evolution of W and ω is considered. Flux-surface averages are obtained by integrating in space between neighbouring surfaces. For quantities which fux-surface average to zero, a further refinement in the spatial integration is obtained by introducing smaller cells in the ξ-direction (Fig. 1).

4. Numerical results

In the numerical simulations, ITER-relevant parameters have been employed: major radius $R =$ 8 m, magnetic field $B_0 = 8$ T, deuterium plasma with density $n_i = 10^{20}$ m^{-3}, temperature $T_i = 5$ keV. A flat background pressure profile is taken and no bootstrap current is generated. The only contribution to the parallel flow is then due to the island electric field. Since the perpendicular current is zero when flux-surface averaged, it is calculated here as $j_\perp \equiv (j_\perp^{\text{upper}} - j_\perp^{\text{lower}})/2$, where the superscripts refer to the lower (from the X-point to the O-point) and upper (O-point to X-point) part of the island, see Fig. 1. The poloidal and toroidal mode numbers in the simulations are $m = 3$, $n = 2$, respectively.

The consequences of the relaxation of the limitations (1,2) on the allowed island width and rotation frequency which are usually required for an analytic treatment of the NTM dynamics are investigated separately. The behaviour of $j_\perp$ as a function of ω is discussed first. In this case, a "large" island width ($w_b/W \approx 0.1$) is taken. The results of the simulations are shown in Fig. 2, where $j_\perp$ is radially averaged on the island inside and over a region lying within a distance of $3W$ from the island separatrix. Since pressure gradient is zero in these simulations, the polarisation current should scale as $j_\perp \propto \omega^2$, consistently with Eq. (5) and the fact that $\Phi \propto \omega$, Eq. (3). The behaviour of $j_\perp$ is much more complicated, indicating that other physical processes are involved. An analysis of the particle motion in the island potential shows that when the frequency is small ($-0.5 \lesssim \omega/k_{||}v_{\text{th}} \lesssim 0.5$, where in these simulations $k_{||}v_{\text{th}} = 3.9 \cdot 10^3$ s^{-1}) the toroidal drift of the trapped particles cannot be neglected. It turns out that when the toroidal drift has a frequency comparable with the island rotation frequency, a trapped particle can drift away from the perturbed magnetic surface under the influence of the radial component of the $E \times B$ velocity, related to the angular components of the island electric field. A sign reversal in $j_\perp$ is found for $\omega/k_{||}v_{\text{th}} \simeq 0.1$, which corresponds approximately to twice (since $n = 2$) the precession frequency of the thermal ions. This can be seen in Fig. 3a, where the particles with $v/v_{\text{th}} \approx 2.3$ have a toroidal drift frequency $\omega_{td} \approx \omega/2$. When ω increases above this value, the $E \times B$ flow starts to dominate the motion, forcing the trapped particles to follow approximately

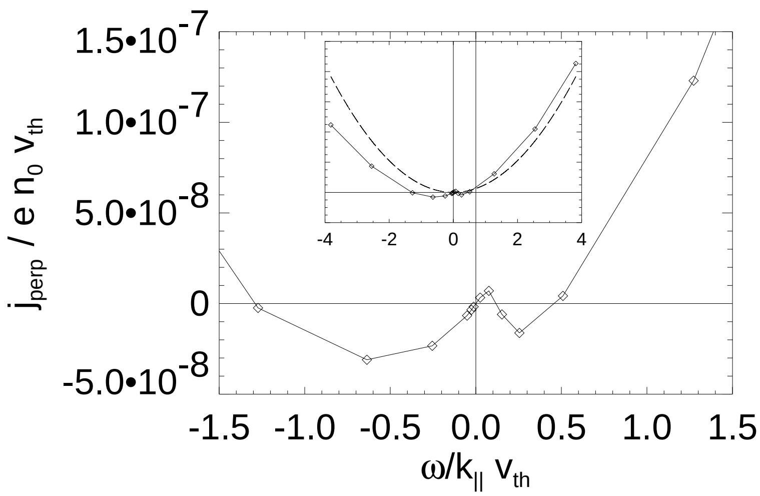

Figure 2: The perpendicular current $j_\perp$ (normalised to $env_{\rm th}$) as a function of the island rotation frequency ω (normalised to the parallel streaming frequency $k_\| v_{\rm th}$). The dashed curve shows the estimate $(\omega r/m)^2/r\omega_c v_{\rm th}$.

the perturbed surfaces and the standard polarisation current (cf. again Fig. 1) sets in. This leads $j_\perp$ towards positive values, until the x axis is crossed on both sides. This second sign reversal is particularly important, because it occurs for values of ω which lie in the range where it is expected to be experimentally, i.e. close to the diamagnetic frequency. This can be seen from Fig. 2, recalling that $\omega_*/k_\| v_\| = (\rho_p/W)(L_q/L_n)$, which is close to unit, at least when the island is not fully developed. This transition is not captured by a fluid approach, or by a kinetic treatment in a slab geometry. It is also interesting to notice that in the range where the “standard” polarisation current is found, ω starts to be comparable to the bounce freuency of the ions ω_b, in particular the slower ones. In fact, it is seen in the simulations that thermal particles start to drive $j_\perp$ to positive values in Fig. 2 at smaller values of ω when compared to suprathermal (Fig. 3b). A Fourier analysis of the motion shows the interference of the two periodic motions.

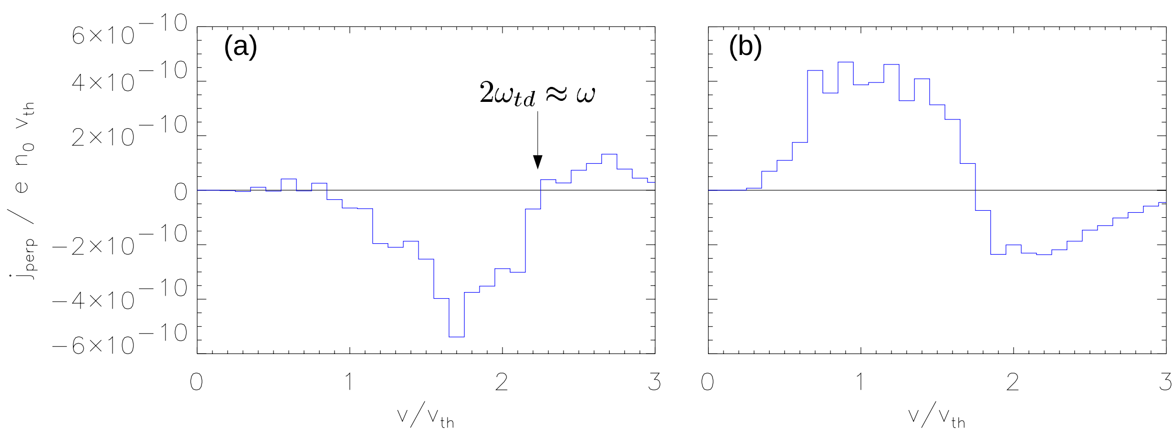

Figure 3: Velocity distribution of the perpendicular current $j_\perp$ in the first outer cell after the island separatrix for $\omega/k_\| v_{\rm th} = 0.15$ (a) and $\omega/k_\| v_{\rm th} = 0.51$ (b).

Finally, for very high island frequencies, particles with $\omega_b \lesssim \omega$ are seen to reverse again their contribution to $j_\perp$. It is recalled that the polarisation current contributes to the island evolution through its parallel closure, which can be obtained by integrating the continuity equation $\nabla_\| j_\| = -\nabla_\perp \cdot \mathbf{j}_\perp$. If one evaluates the sign of the contribution of the polarisation current (when

$j_\perp \propto \omega^2$) to the island stability using the simulated radial profiles and the previous equation, it turns out that the polarisation current is stabilising if the region across the island separatrix is excluded from the radial integration, while it destabilising if it is included, according to the present theoretical understanding [15]. Moreover, applying similar considerations to the $j_\perp$-profiles corresponding to the sign reversal discussed above, one can deduce that the different sign of $j_\perp$ should correspond to a different sign of $j_{||}$, implying a different contribution of the polarisation current to Eq.(7).

The dipendence of the perpendicular current as a function of the island width W has been studied taking ω in the frequency range where the $j_\perp \propto \omega^2$, i.e. where the standard polarisation current dominates. The parallel flux which develops as a consequence of the neoclassical damping of the poloidal rotation (see Sec. 2) behaves, when W is reduced down to the order of the banana width w_b, in a way which reminds the scaling of the bootstrap current in the same situation [16]. This can be easily understood since the physics governing the two phenomena is very similar. It is found that the trapped particles drifting close to the island can cross its separatrix, so that they move according to an averaged potential (or, in the case of the bootstrap current, an averaged pressure), which changes across the separatrix according to Eqs. (3,4). In a reference frame moving with the island, the electric potential is proportional to the function $h(\Omega)$ and vanishes inside the separatrix. Therefore, when the orbit width of the trapped particles is comparable to the island width W and the particle drift significantly into the island, the polarisation drift is reduced, as shown in Fig. 4. In the standard theory ($W \gg w_b$), $j_\perp$ does not dipend on W,

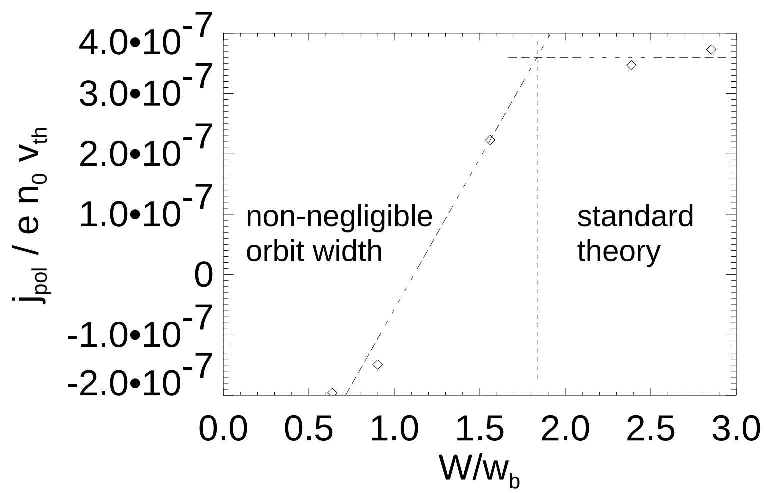

Figure 4: Polarisation current reduction for island widths W comparable to the ion banana width w_b.

as discussed in Sec. 2. The reduction of the polarisation current results to scale linearly with W/w_b. A sign flip of $j_\perp$ is found in these simulations to occurr at about $W \approx w_b$, due to the contribution coming from inside the island. Again, one can try to evaluate the effect of this behaviour on $j_{||}$ from the continuity equation. A preliminar analysis indicates that $j_{||}$ follows the behaviour of $j_\perp$, leading to a reduction of its contribution in the Rutherford equation and possibly even to a sign reversal for very small island widths.

5. Conclusions

The polarisation current due to a rotating magnetic island has been studied in this paper employing drift kinetic δf simulations. The numerical approach enables one to investigate a broader parameter range than allowed by the analytic 3D theory. Only the ions are described by the simulation markers, and the potential is prescribed. The electrons just short-circuit the parallel electric field. An extension of the analysis to include self consistent potentials and the electron dynamics would be very interesting and is planned for the future.

The two issues investigated in this paper, namely the variation of $j_\perp$ with the island frequency ω and the island width W, show that a complete kinetic description of the particle dynamics in toroidal geometry is indispensable in order to obtain a reliable calculation of the polarisation current. A sign reversal, not predicted by the fluid theory, has been found for frequencies close to the diamagnetic frequency even in the absence of a pressure gradient. Moreover, the size of the current is usually overestimated in the analysis of the mode evolution, since it decreases when the island width is comparable to the ion banana width. These results point towards a reduction of the role the polarisation current in the evolution of the NTM. However, a contribution to the determination of the NTM threshold cannot be excluded.

References

[1] FURTH, H. P. et al., Physics of Fluids **6** (1963) 459.
[2] RUTHERFORD, P. H., Physics of Fluids **16** (1973) 1903.
[3] QU, W. X. et al., University of Wisconsin Plasma Report **UWPR 85-5** (1985).
[4] CARRERA, R. et al., Physics of Fluids **29** (1986) 899.
[5] CHANG, Z. et al., Physical Review Letters **74** (1995) 4663.
[6] SAUTER, O. et al., Physics of Plasmas **4** (1997) 1654.
[7] ZOHM, H., Physics of Plasmas **4** (1997) 3433.
[8] SMOLYAKOV, A. I. et al., Physics of Plasmas **2** (1995) 1581.
[9] WILSON, H. R. et al., Physics of Plasmas **3** (1996) 248.
[10] MIKHAILOVSKII, A. B., Contributions to Plasma Physics **43** (2003) 125.
[11] POLI, E. et al., Plasma Physics and Controlled Fusion **45** (2003) 71.
[12] HINTON, F. L. et al., Physics of Fluids **27** (1984) 1243.
[13] BERGMANN, A. et al., Physics of Plasmas **8** (2001) 5192.
[14] PINCHES, S. D. et al., Computer Physics Communications **111** (1998) 133.
[15] WAELBROECK, F. L. et al., Physical Review Letters **78** (1997) 1703.
[16] POLI, E. et al., Physical Review Letters **88** (2002) 075001.